

## Transport properties of vanadium germanate glassy semiconductors

Aswini Ghosh

*Indian Association for the Cultivation of Science, Jadavpur, Calcutta 700 032, West Bengal, India*

(Received 5 March 1990)

Measurements are reported for the dc as well as frequency-dependent (ac) conductivities (real and imaginary parts) for various compositions of the vanadium germanate glassy semiconductors in the temperature range 80–450 K. The experimental results are analyzed with reference to various theoretical models proposed for electrical conduction in amorphous semiconductors. The analysis shows that at high temperatures the temperature dependence of the dc conductivity is consistent with Mott's model of phonon-assisted polaronic hopping conduction in the adiabatic approximation, while the variable-range-hopping mechanism dominates at lower temperatures. Schnakenberg's model predicts the temperature dependence of the observed activation energy in the intermediate temperature range. The temperature dependence of the ac conductivity is consistent with the simple quantum-mechanical tunneling model at lower temperatures, although this model cannot predict the observed temperature dependence of the frequency exponent. The overlapping-large-polaron tunneling model can explain the temperature dependence of the frequency exponent at low temperature; however, this model predicts a temperature dependence of the ac conductivity much higher than the observed data show. On the other hand, the correlated-barrier-hopping model is consistent with the temperature dependence of both the ac conductivity and its frequency exponent over the entire temperature range of measurements.

### I. INTRODUCTION

Oxide glasses containing transition-metal ions (TMI's) show semiconducting behavior due to the presence of TMI's in multivalent states in the glassy matrices<sup>1,2</sup> (e.g., V<sup>4+</sup> and V<sup>5+</sup> in vanadate and Cu<sup>+</sup> and Cu<sup>2+</sup> in cuprate glasses). It is generally agreed that the dc electrical conduction in these glassy semiconductors takes place by the hopping movement of small polarons between TMI sites of different valence states.<sup>1–6</sup> The activation energy for dc conduction is observed to be temperature dependent.<sup>1–6</sup> It is also observed that the frequency-dependent ac conductivity shows an approximately linear frequency dependence at low frequencies and temperatures.<sup>3,7–11</sup> Several studies<sup>3,5–11</sup> were performed on the dc and ac conduction in these TMI glassy semiconductors. However, fewer attempts<sup>6–11</sup> were made for comparative studies in light of various existing theories<sup>1,2,12,13</sup> proposed for electrical conduction in amorphous semiconductors.

The purpose of the present work is to investigate the dc as well as the frequency-dependent (ac) complex conductivity of various compositions of vanadium germanate glassy semiconductors with the help of various existing theories over the temperature range 80–450 K. Various theoretical models proposed for the dc and ac conduction in amorphous semiconductors are briefly described in Sec. II. Section III includes the experimental procedure. The results are presented in Sec. IV and are analyzed in Sec. V with the help of the models described in Sec. II.

### II. THEORY

Many different theories<sup>1,2,12,13</sup> have been proposed for the dc as well as ac conduction processes in amorphous

semiconductors. To compare the various theories with the experimental data, the detailed predictions of these theories need to be examined and thus each approach is discussed below briefly.

#### A. dc conduction

Mott<sup>1</sup> has investigated a conduction model for TMI glasses, in which the conduction process is considered in terms of phonon-assisted hopping of small polarons between localized states. The dc conductivity in the Mott model for the nearest-neighbor hopping in the high-temperature limit ( $T > \Theta_D/2$ ) is given by<sup>1</sup>

$$\sigma = \nu_0 [e^2 C(1-C)/k_B T R] \exp(-2\alpha R) \exp(-W/k_B T), \quad (1)$$

where  $\nu_0$  is the longitudinal optical phonon frequency,  $R$  is the average site separation,  $\alpha^{-1}$  is the spatial decay parameter for the  $s$ -like wave function assumed to describe the localized state at each site,  $C$  is the fraction of sites occupied by an electron (or polaron) (and therefore is the ratio of the TMI concentration in the low valence state to the total TMI concentration), and  $W$  is the activation energy for dc conduction.

Assuming that a strong electron-phonon interaction exists, the activation energy  $W$  is the result of polaron formation with binding energy  $W_p$  and an energy difference  $W_D$  which might exist between the initial and final sites due to variations in the local arrangements of ions. Austin and Mott<sup>2</sup> have shown that

$$W \simeq \begin{cases} W_H + W_D/2 & \text{for } T > \Theta_D/2 \\ W_D & \text{for } T < \Theta_D/4, \end{cases} \quad (2a)$$

where  $W_H$  ( $\approx \frac{1}{2}W_p$ ) is the polaron hopping energy and  $\Theta_D$ , defined by  $h\nu_0 = k_B\Theta_D$ , is the characteristic Debye temperature. It should be noted that Eq. (1) for the dc conductivity in the Mott model is for hopping of polarons in the nonadiabatic regime. However, the tunneling term  $\exp(-2\alpha R)$  reduces to unity for hopping in the adiabatic limit. An estimate of polaron hopping energy  $W_H$  is also given by Mott,<sup>2</sup>

$$W_H = e^2/4\epsilon_p r_p, \quad (2b)$$

where  $r_p$  is the small polaron radius and  $\epsilon_p$  is an effective dielectric constant.

At lower temperatures ( $T < \Theta_D/4$ ), where polaron binding energy is small and the disorder energy (here  $W_D$ ) plays a dominant role in the conduction mechanism, Mott<sup>14,15</sup> has proposed that hop may occur preferentially beyond nearest neighbors. The conductivity for the so-called "variable range hopping" is predicted to be

$$\sigma = A \exp(-B/T^{1/4}), \quad (3a)$$

where  $A$  and  $B$  are constants and  $B$  is given by

$$B = 2.1[\alpha^3/k_B N(E_F)]^{1/4}, \quad (3b)$$

where  $N(E_F)$  is the density of states at the Fermi level. Thus the variable-range-hopping model predicts a  $T^{-1/4}$

dependence of the logarithmic dc conductivity at low temperatures. Similar temperature dependence of the dc conductivity at low temperatures was also obtained by Ambegaokar and co-workers<sup>16</sup> on the basis of percolation model.

For the case  $W_D = 0$ , a generalized polaron model has been investigated in detail by Holstein,<sup>17</sup> Emin and Holstein,<sup>18</sup> and Friedman and Holstein<sup>19</sup> covering both the adiabatic and nonadiabatic hopping processes. On the basis of molecular crystal model, Friedman and Holstein<sup>19</sup> have derived an expression for the dc conductivity,

$$\sigma = \frac{3}{2}(e^2 N R^2 J^2 / k_B T)(\pi / k_B T W_H)^{1/2} \exp(-W_H / k_B T) \quad (4)$$

for the case of nonadiabatic hopping, while Emin and Holstein<sup>18</sup> have shown that in the case of adiabatic regime,

$$\sigma = \frac{8\pi}{3}(N e^2 R^2 \nu_0 / k_B T) \exp[-(W_H - J) / k_B T], \quad (5)$$

where  $N$  is the site concentration and  $J$  is a polaron bandwidth related to electron wave-function overlap on adjacent sites. The condition for the nature of hopping has also been proposed and is expressed by<sup>17</sup>

$$J \begin{cases} > \\ < \end{cases} \left\{ (2k_B T W_H / \pi)^{1/4} (h\nu_0 / \pi)^{1/2} \right\} \begin{cases} \text{for adiabatic hopping} \\ \text{for nonadiabatic hopping} \end{cases} \quad (6)$$

with the condition for the existence of a small polaron being  $J \leq W_H/3$ .

Schnakenberg<sup>20</sup> has considered a more-general polaron hopping model where  $W_D \neq 0$ . In his model, optical multiphonon process determines the dc conductivity at high temperatures, while at low temperatures charge-carrier transport is an acoustical one-phonon-assisted hopping process. The temperature dependence of the dc conductivity in the Schnakenberg model has the form

$$\begin{aligned} \sigma &\sim T^{-1} [\sinh(h\nu_0/k_B T)]^{1/2} \\ &\times \exp[-(4W_H/h\nu_0) \\ &\times \tanh(h\nu_0/4k_B T)] \exp(-W_D/k_B T). \end{aligned} \quad (7a)$$

It is noted that Eq. (7a) predicts a temperature-dependent hopping energy given by

$$W'_H = W_H [\tanh(h\nu_0/4k_B T)] / (h\nu_0/4k_B T). \quad (7b)$$

Equation (7b) shows a decrease of activation energy with decrease of temperature.

Killias<sup>21</sup> has proposed a polaron model in which the variation of activation energy is considered to be due to thermally activated hopping in a system which has a distribution of hopping distances. Assuming a Gaussian distribution for the hopping distances centered around a median value  $R_0$ , Killias has obtained the following expression for the dc conductivity:

$$\begin{aligned} \sigma &= A \exp[-W(R_0)/k_B T - (a/2\beta k_B T)^2] \\ &\times [1 - \frac{1}{2} \operatorname{erfc}(\beta R_0 - a/2\beta k_B T)], \end{aligned} \quad (8)$$

where  $A$  is a constant,  $a = dW/dR$ , and  $\beta^{-1}$  is proportional to the width of the Gaussian distribution. Equation (8) predicts a nonlinear behavior of the dc conductivity which may be described most conveniently by a temperature-dependent activation energy<sup>21</sup> given by

$$W(T) = W_0(1 - \Theta_R/T), \quad (9a)$$

where  $W_0$  and  $\Theta_R$  are constants and  $\Theta_R$  is given by

$$\Theta_R \approx a^2/4\beta k_B W_0. \quad (9b)$$

## B. ac conduction

A frequency-dependent ac conductivity  $\sigma(\omega)$  has been observed in many amorphous semiconductors and insulators<sup>15</sup> (both inorganic and polymeric organic materials), and invariably has the form

$$\sigma(\omega) = A\omega^s, \quad (10)$$

where  $A$  is a constant dependent on temperature,  $\omega$  is the (circular) frequency, and the exponent  $s$  is generally less than or equal to unity. All that is required to show this behavior is that the loss mechanism should have a very wide range of possible relaxation times,  $\tau$ . In particular,

an approximately linear frequency dependence of  $\sigma(\omega)$  is predicted if the distribution of relaxation times,  $n(\tau)$ , is inversely proportional to  $\tau$ , which results if  $\tau = \tau_0 \exp(\zeta)$ , where  $\zeta$  is a random variable and  $\tau_0$  a characteristic relaxation time, often taken to be an inverse phonon frequency,  $\nu_0^{-1}$ . Any departures from linearity carry information on the particular type of loss mechanism involved. It should be noted that what is measured in a given ac experiment is the total conductivity  $\sigma_{\text{tot}}(\omega)$  of the sample at a particular frequency and temperature. In general, this can be written as

$$\sigma_{\text{tot}}(\omega) = \sigma(\omega) + \sigma, \quad (11)$$

where  $\sigma$  is, as before, the dc conductivity, and it is tacitly assumed that the dc and ac conductivities are due to completely different processes. However, when the dc and ac conductivities arise due to the same process and  $\sigma$  is simply  $\sigma(\omega)$  in the limit  $\omega \rightarrow 0$ , then the separation given in Eq. (11) is no longer valid.

Various theories<sup>12,13</sup> for ac conduction in amorphous semiconductors have been proposed. It is commonly assumed that the pair approximation holds, namely the dielectric loss occurs due to the carrier motion considered to be localized within pairs of sites. In essence, two distinct processes have been proposed for the relaxation mechanism, namely quantum-mechanical tunneling and classical hopping over a barrier, or some combination or variant of the two, and it has been variously assumed that electrons (or polarons) or atoms are the carriers responsible.

For the quantum-mechanical tunneling (QMT) model, the random variable is  $\zeta = 2\alpha R$ , where  $\alpha$  and  $R$  have the same meaning as before and it is commonly assumed that  $\alpha$  is constant for all sites. Several authors<sup>2,13,22-25</sup> have evaluated, within the pair approximation, the real part [denoted by  $\sigma_1(\omega)$ ] of the ac conductivity for single electron motion undergoing QMT and obtained the expression

$$\sigma_1(\omega) = C^1 e^2 k_B T \alpha^{-1} [N(E_F)]^2 \omega R_\omega^4, \quad (12)$$

where  $C^1$  is a numerical constant that varies slightly according to different authors, but may be taken as  $\pi^4/24$  (cf., Ref. 13, 23, and 25).  $R_\omega$  is the hopping distance at a particular frequency  $\omega$ , given by

$$R_\omega = (2\alpha)^{-1} \ln(1/\omega\tau_0). \quad (13)$$

The frequency dependence of  $\sigma_1(\omega)$  in the form of Eq. (10) can be deduced using the relation

$$s = d \ln \sigma_1(\omega) / d \ln \omega \quad (14)$$

and for the QMT model [Eq. (12)] this gives

$$s = 1 - 4 / \ln(1/\omega\tau_0). \quad (15)$$

The above results are obtained in a wide band limit, i.e., for  $\Delta_0 \gg k_B T$ , where  $\Delta_0$  is the bandwidth. Thus, for the QMT model the frequency exponent  $s$  is temperature independent but frequency dependent, and for typical values of the parameters, namely,  $\tau_0 \approx 10^{-13}$  s and  $\omega = 10^4$  s<sup>-1</sup>, a value of  $s \approx 0.81$  is deduced from Eq. (15).

A temperature-dependent frequency exponent can be obtained within the framework of the QMT model in the pair approximation by assuming that the carriers form nonoverlapping small polarons. Transport of an electron between degenerate sites having a random distribution of separations will, therefore, generally involve an activation energy, the polaron hopping energy  $W_H \approx W_p/2$ . In this case the frequency exponent becomes<sup>12</sup>

$$s = 1 - 4 / [\ln(1/\omega\tau_0) - W_H/k_B T]. \quad (16)$$

Now it is noted that  $s$  is temperature dependent, increasing with increasing temperature. It should also be noted that a temperature-dependent frequency exponent can arise from the simple QMT model if pair approximation breaks down, i.e., when the carrier motion occurs within clusters.<sup>26</sup> The tunneling distance  $R_\omega$  is the nonoverlapping small polaron (NSPT) model becomes

$$R_\omega = (2\alpha)^{-1} [\ln(1/\omega\tau_0) - W_H/k_B T] \quad (17)$$

and the ac conductivity in the NSPT model is given by Eq. (12) with the above expression [Eq. (17)] for  $R_\omega$ . The behavior of this model might, at first sight, appear to be pathological in that  $s$  can apparently become infinity at sufficiently high frequency and/or low temperatures due to the hopping length  $R_\omega \rightarrow 0$ , when the term in the square bracket in the above expression [Eq. (17)] for  $R_\omega$  tends to zero. In practice, of course, the minimum value of  $R_\omega$  is equal to the interatomic spacing; for higher frequencies or temperatures lower than those given by the critical conditions, the contribution to the overall ac conductivity due to small polaron tunneling mechanism tends toward zero.

Long<sup>13</sup> has proposed a mechanism for the polaron tunneling model where the large polaron wells of the two sites overlap, thereby reducing the value of polaron hopping energy,<sup>2,26</sup> i.e.,

$$W_H = W_{\text{HO}}(1 - r_0/R), \quad (18)$$

where  $r_0$  is the overlapping large polaron radius. It is assumed that  $W_{\text{HO}}$  is constant for all sites, whereas intersite separation  $R$  is a random variable. The real part of the ac conductivity for the overlapping-large-polaron tunneling (OLPT) model<sup>13</sup> is given by

$$\sigma_1(\omega) = \frac{\pi^4 e^2 (k_B T)^2 [N(E_F)]^2 \omega R_\omega^4}{12 2\alpha k_B T + W_{\text{HO}} r_0 / R_\omega^2}, \quad (19)$$

where the hopping length  $R_\omega$  is determined by the quadratic equation

$$(R'_\omega)^2 + [(W_{\text{HO}}/k_B T) + \ln(\omega\tau_0)] R'_\omega - W_{\text{HO}} r'_0 / k_B T = 0, \quad (20)$$

where

$$R'_\omega = 2\alpha R_\omega \quad \text{and} \quad r'_0 = 2\alpha r_0.$$

The frequency exponent of  $\sigma_1(\omega)$  in this model can be evaluated as

$$s = 1 - \frac{8\alpha R_\omega + 6W_{\text{HO}}r_0/R_\omega k_B T}{(2\alpha R_\omega + W_{\text{HO}}r_0/R_\omega k_B T)^2} \quad (21)$$

Thus the OLPT model predicts that  $s$  should be both temperature and frequency dependent. It can also be seen from Eq. (21) that  $s$  decreases from unity with increasing temperature. For large values of  $r'_0$ ,  $s$  continues to decrease with increasing temperature, eventually tending to the value of  $s$  predicted by the simple QMT model, whereas for small values of  $r'_0$ ,  $s$  exhibits a minimum<sup>13</sup> at a certain temperature and subsequently increases with increasing temperature in a similar fashion to the case of NSPT model.

The other type of process, which has been proposed for the relaxation mechanism, is the classical hopping over a barrier (HOB), where the random variable is  $\zeta = W/k_B T$ . For the case of atomic motion the following expression is obtained<sup>13,27</sup> for the ac conductivity:

$$\sigma_1(\omega) = \frac{\pi}{3} \eta (Np^2 k_B T / W_0 \Delta_0) \omega \tanh(\Delta_0 / 2k_B T), \quad (22)$$

where  $\eta$  is a meanfield correction term,  $N$  is the number of pair states per unit volume,  $p$  is the dipole moment associated with the transition, and it is assumed that the energy difference between sites,  $\Delta$ , is randomly distributed in the range  $0 < \Delta < \Delta_0$  and the barrier height is also randomly distributed in the range  $0 < W < W_0$ . It is noted from Eq. (22) that for this simple HOB model the frequency exponent of  $\sigma_1(\omega)$  is predicted to be unity and is independent of temperature and frequency. It might be mentioned here that for the case of atomic tunneling, an expression similar to Eq. (22) is obtained<sup>28</sup> again with  $s = 1$ , if the dipole moment is uncorrelated with the hopping distance.<sup>13</sup>

A model for the ac conduction, which correlates the relaxation variable  $W$  with the intersite separation  $R$ , has been developed initially by Pike<sup>29</sup> for single electron hopping and extended by Elliott<sup>12,30</sup> for two electrons hopping simultaneously. For neighboring sites at a separation  $R$ , the Coulomb wells overlap, resulting in a lowering of the effective barrier height from  $W_M$  to a value  $W$ , which for the case of one electron transition is given by<sup>29</sup>

$$W = W_M - e^2 / \pi \epsilon \epsilon_0 R, \quad (23)$$

where  $\epsilon$  is the dielectric constant of the material and  $\epsilon_0$  that of free space. The ac conductivity (real part) in this model, called the ‘‘correlated barrier hopping’’ (CBH) model, in the narrow band limit ( $\Delta_0 \ll k_B T$ ) is expressed by

$$\sigma_1(\omega) = \frac{\pi^3}{24} N^2 \epsilon \epsilon_0 \omega R^6, \quad (24)$$

where  $N$  is the concentration of pair sites and  $R_\omega$  is the hopping distance given by

$$R_\omega = e^2 / \pi \epsilon \epsilon_0 [W_M + k_B T \ln(\omega \tau_0)]. \quad (25)$$

The frequency exponent  $s$  for this model is evaluated as<sup>12</sup>

$$s = 1 - 6k_B T / [W_M + k_B T \ln(\omega \tau_0)]. \quad (26)$$

Thus, in the CBH model a temperature-dependent exponent is predicted, with  $s$  increasing towards unity as  $T$  tends to zero, in marked contrast to the QMT or simple HOB mechanism. In the broad-band, i.e., low-temperature limit ( $\Delta_0 \gg k_B T$ ),  $N$  in Eq. (24) is replaced by  $Nk_B T / \Delta_0$  and so an additional  $T^2$  dependence of  $\sigma_1(\omega)$  is introduced.<sup>13</sup> It should be noted that for the two-electron CBH model,<sup>12,30</sup> expressions (24) and (25) for  $\sigma_1(\omega)$  and  $R_\omega$ , respectively, are multiplied by 2, but the expression (26), for  $s$ , however, remains unaltered.

It might appear that the behavior of the CBH model is also pathological in the same sense as discussed previously for the NSPT model. In this case, however, when the denominator of Eq. (25) tends to zero,  $R_\omega$  tends to infinity. However, long before this can occur, the pair approximation breaks down and the dc percolation limit is reached with the result that the CBH model is no longer valid.<sup>12</sup>

Several developments<sup>31,32</sup> of this theory have been made. The assumption of randomly distributed centers used in the derivation of Eq. (24) has been relaxed for the case of melt-quenched chalcogenide glasses where pairing of charged defects may occur. The result of this is an enhancement of the frequency exponent  $s$  [Eq. (26)] by an additional term  $T/8T_g$ , where  $T_g$  is the glass transition temperature.

Thus far, the real part [ $\sigma_1(\omega)$ ] of the ac conductivity has been discussed only, neglecting the imaginary part [denoted by  $\sigma_2(\omega)$ ] of the ac conductivity, which is related to the dielectric constant. Although the real and imaginary parts of the conductivity are related via the Kramers-Kronig relation, valuable information can be lost if  $\sigma_2(\omega)$  is neglected, because the models for ac conduction also make specific predictions concerning the dielectric constant, and the comparison of theory and experiment is straightforward, since the capacitance measurements are inherently much more accurate than conductance measurements when made using a conventional bridge technique.

It has been shown<sup>13</sup> that the ratio of the imaginary to the real part of the ac conductivity has a characteristically different functional form for the various mechanism of dielectric relaxation described above. For the simple QMT model, it is predicted that

$$\sigma_2(\omega) / \sigma_1(\omega) = -(2/5\pi) \ln(\omega \tau_0), \quad (27)$$

while for the NSPT model,

$$\sigma_2(\omega) / \sigma_1(\omega) = -(2/5\pi) \ln(\omega \tau_0) \times [1 + W_H / k_B T \ln(\omega \tau_0)]. \quad (28)$$

The CBH model<sup>13</sup> predicts to a first approximation (i.e., for small  $k_B T / W_M$ )

$$\sigma_2(\omega) / \sigma_1(\omega) = -(2/\pi) \ln(\omega \tau_0) \times [1 + (3k_B T / W_M) \ln(\omega \tau_0)]. \quad (29)$$

It may be noted that Eqs. (29) and (28) predict a temperature dependence for  $\sigma_2(\omega) / \sigma_1(\omega)$ , while Eq. (27) does not. For the OLPT model,  $\sigma_2(\omega) / \sigma_1(\omega)$  behaves like

that for the simple QMT model at high temperatures, whereas at low temperatures the behavior is similar to that exhibited by the CBH model.

### III. EXPERIMENTAL PROCEDURE

The glassy samples (Table I) were prepared by melting the reagent-grade  $V_2O_5$  and  $GeO_2$  in alumina crucibles at 1273 K for 2 h in air atmosphere. The melt was quenched between two polished brass plates held at room temperature.

The amorphous nature of the samples was confirmed by x-ray-diffraction (Philips, model PW 1050) and scanning electron microscopy (Hitachi, model S-415A) studies. The scanning electron micrographs also showed homogeneous character of the samples.

The final sample composition and the concentrations of total vanadium ions ( $[V^{5+}] + [V^{4+}]$ ) were determined by atomic absorption spectroscopy (Varian, model AA 1745). The concentrations of the reduced vanadium ions ( $[V^{4+}]$ ) were estimated from ESR spectra obtained using a Varian E-12 X-band spectrometer. A spectrum of a single crystal of  $CuSO_4 \cdot 5H_2O$  was used as a standard. The density of the samples was determined by Archimedes' principle. The average intersite separation ( $R$ ) was obtained from the final composition and density. The final sample compositions, the ratio  $C = [V^{4+}] / ([V^{5+}] + [V^{4+}])$ , and other physical parameters are shown in Table I.

For electrical measurements, disk-shaped samples of diameter  $\sim 8-10$  mm and thickness  $0.5-1.0$  mm were cut and polished. The dc conductivity of the samples was measured using a Keithley 617 electrometer. Before measurements, Ohmic behavior at the contacts was ascertained from the linearity of the  $I-V$  characteristics. The ac measurements were carried out in a General Radio (model GR-1615A) capacitance bridge, which measures equivalent parallel conductance and capacitance of a sample for frequencies ( $\omega/2\pi$ ) between 20 and  $10^5$  Hz in a three-terminal arrangement. Evaporated gold electrode was used for both the dc and ac measurements. An evacuable chamber was employed as a sample cell and was inserted inside a cryostat for low-temperature measurements. Measurements were made in the temperature range 80–450 K with a stability of  $\pm 0.5$  K.

### IV. RESULTS

The dc conductivity  $\sigma$  of the various sample compositions is shown in Fig. 1 as a function of reciprocal tem-

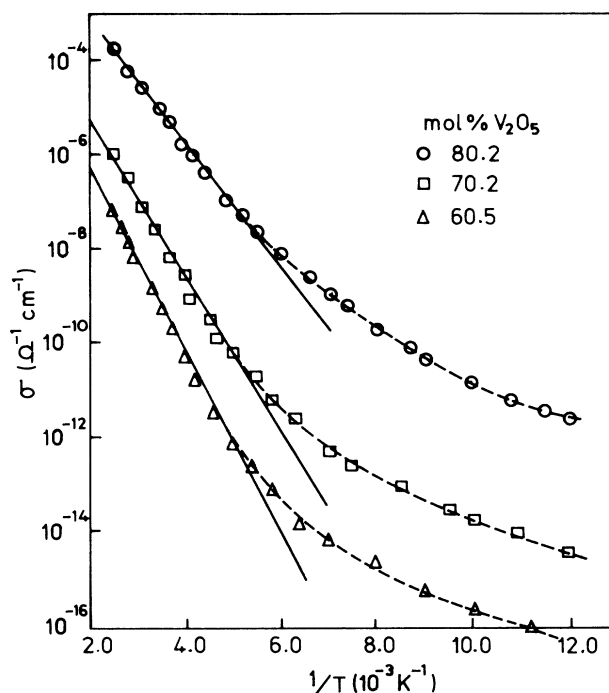


FIG. 1. The dc conductivity shown as a function of reciprocal temperature for three sample compositions shown. The solid lines are fits to Eq. (1) predicted by Mott's model. The dashed curves are drawn through the data.

perature. It is clear from Fig. 1 that the dc conductivity shows an activated behavior above  $\sim 200$  K. However, below 200 K the behavior of the dc conductivity is non-linear, indicating a temperature-dependent activation energy. The activation energy decreases with decreasing temperature.

Figure 2 shows the measured total conductivity  $\sigma_{tot}(\omega)$  as a function of reciprocal temperature at various frequencies for one glass composition, along with the dc conductivity  $\sigma$ . It is evident that the temperature dependence of  $\sigma_{tot}(\omega)$  is much less than that of  $\sigma$  at low temperatures and is not activated in behavior. However, at higher temperatures the temperature dependence of  $\sigma_{tot}(\omega)$  becomes strong and its frequency dependence becomes small. Other sample compositions also showed similar behavior.

The measured total conductivity  $\sigma_{tot}(\omega)$  as a function of frequency at various temperatures is shown in Fig. 3(a) for the same sample composition as in Fig. 2. It is also

TABLE I. Analyzed sample compositions, concentrations of the total and reduced vanadium ions, their ratios, and average intersite separation for the vanadium germanate glassy semiconductors.

Analyzed compositions (mol %)		Density (g cm <sup>-3</sup> )	[V <sup>5+</sup> ] + [V <sup>4+</sup> ] (cm <sup>-3</sup> )	[V <sup>4+</sup> ] (cm <sup>-3</sup> )	C	R (Å)
V <sub>2</sub> O <sub>5</sub>	GeO <sub>2</sub>					
80.2	19.9	3.08	$1.65 \times 10^{22}$	$1.32 \times 10^{21}$	0.08	3.93
70.2	29.8	2.95	$1.52 \times 10^{22}$	$1.52 \times 10^{21}$	0.10	4.04
60.5	39.5	2.80	$1.39 \times 10^{22}$	$2.08 \times 10^{21}$	0.15	4.16

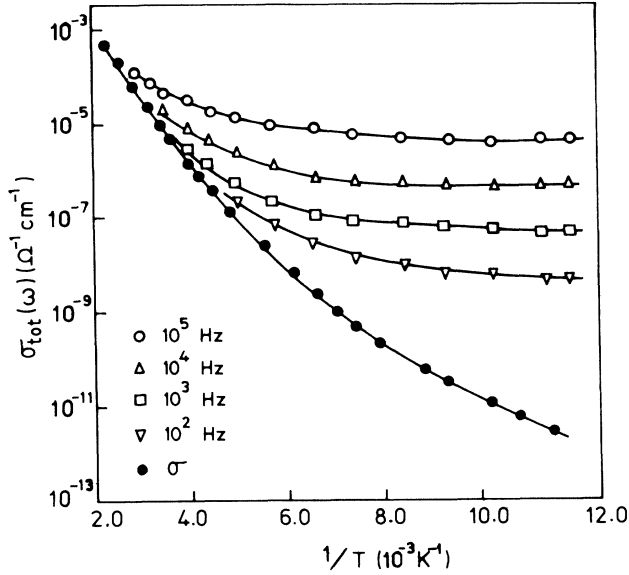


FIG. 2. Measured total conductivity for the sample composition 80.2 mol %  $\text{V}_2\text{O}_5$ –19.8 mol %  $\text{GeO}_2$  shown as a function of reciprocal temperature at four frequencies (shown). The measured dc conductivity is also shown for comparison.

observed that the dc contribution is significant at low frequencies and high temperatures, while the frequency-dependent term dominates at high frequencies and low temperatures. Figure 3(b) shows the frequency-dependent (ac) conductivity,  $\sigma_1(\omega)$  (real part), obtained by subtracting the dc conductivity from the measured conductivity in accordance with Eq. (11), as a function of frequency at the same temperatures and for the same sample composition as in Fig. 3(a). The solid lines in Fig. 3(b) are the straight-line fits obtained by the least-squares-fitting procedure. The frequency exponent  $s$  was also computed from the least-squares fit. Figure 4 depicts the temperature dependence of the frequency exponent  $s$  for various sample compositions. From this figure it is clear that the frequency exponent decreases smoothly with increasing temperature, and also with the increase of vanadium ion concentration in the glass. In the investigated frequency range, frequency dependence of the frequency exponent  $s$  was not observed, even at high temperatures [Fig. 3(b)].

## V. DISCUSSION

### A. dc conductivity

The Mott model for the phonon-assisted hopping of small polarons [Eq. (1)] is consistent with the dc conductivity data presented in Fig. 1 in the high-temperature region. Equation (1) predicted by the Mott model is fitted in Fig. 1 with the experimental data in the high-temperature region, using  $\nu_0$ ,  $\alpha$ , and  $W$  as variable parameters. The best fits are obtained above 200 K for those values of  $\nu_0$ ,  $\alpha$ , and  $W$  shown in Table II. The values of  $\alpha$  are reasonable for localized states and indicate strong localization in the vanadium germanate

TABLE II. Parameters obtained by fitting the high-temperature dc data to the Mott model.

Compositions (mol %)	$W$ (eV)	$\nu_0$ ( $\text{s}^{-1}$ )	$\alpha$ ( $\text{\AA}^{-1}$ )
$\text{V}_2\text{O}_5$			
80.2	0.32	$11 \times 10^{12}$	1.11
70.2	0.39	$10 \times 10^{12}$	1.07
60.5	0.44	$8 \times 10^{12}$	1.04

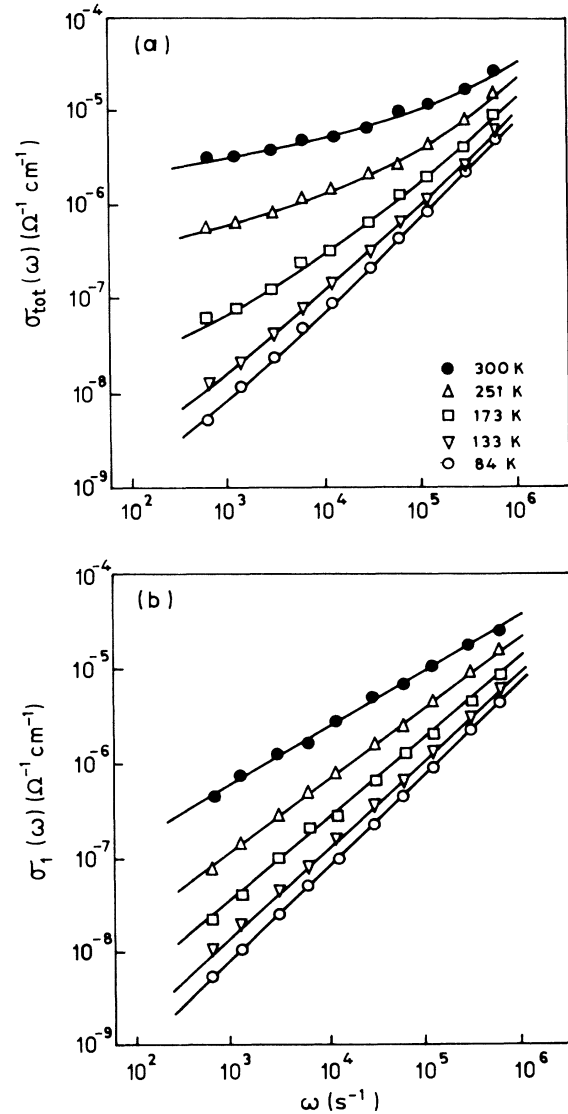


FIG. 3. (a) Frequency dependence of the measured total conductivity for the sample composition 80.2 mol %  $\text{V}_2\text{O}_5$ –19.8 mol %  $\text{GeO}_2$  at several temperatures shown. The solid curves in the figures are fits made using the ac conductivity from the CBH model [Eq. (24)] and the measured value of the dc conductivity. (b) The frequency-dependent conductivity (real part) obtained by subtracting the dc conductivity from the data shown in (a). The solid lines are the straight-line fits obtained by a least-squares-fitting procedure.

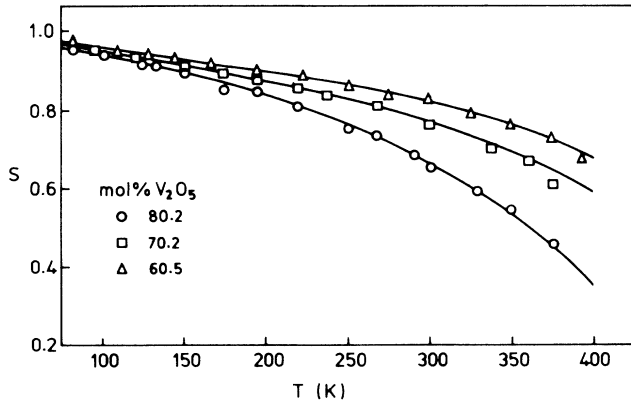


FIG. 4. Temperature dependence of the frequency exponent  $S$  for three sample compositions (shown), obtained by the fitting procedure as in Fig. 3(b). The solid curves in the figure are calculated using the CBH model [Eq. (26)] with the parameters given in Table VIII, assuming a fixed frequency  $\omega = 10^4 \text{ s}^{-1}$ .

glassy semiconductors.<sup>15</sup> The values of the phonon frequency  $\nu_0$  are also reasonable and do not differ appreciably for different glass compositions. These values of  $\nu_0$  are also consistent with the estimate of  $\nu_0$  from infrared studies.<sup>33</sup> The infrared spectra of the various compositions of the vanadium germanate glass<sup>33</sup> are very similar, suggesting that the optical phonon distribution does not differ appreciably between various glass compositions. From these infrared spectra, the characteristic phonon frequency is estimated to be  $\sim 1.1 \times 10^{13} \text{ s}^{-1}$ .

An experimental estimate<sup>2</sup> of the polaron radius  $r_p$  may be obtained within the framework of the Mott model from Eq. (2b), taking  $W \simeq W_H$  and assuming  $W_H \gg J$ . The values obtained are indicated in Table III. The values of  $\epsilon_p$  used in the calculation were obtained from the Cole-Cole plot of complex dielectric constants. Bogomolov *et al.*<sup>34</sup> have shown theoretically that for the case of a nondispersive system of frequency  $\nu_0$  the polaron radius is given by

$$r_p = \frac{1}{2} \left[ \frac{\pi}{6} \right]^{1/3} R, \quad (30)$$

where  $R$  is the site separation. Equation (30) is obviously oversimplified for a complex system, but the infrared spectra of the vanadium germanate system<sup>33</sup> suggest that this approximation may fit the vanadate system fairly well. The values of the polaron radius calculated from

TABLE III. Effective dielectric constant and polaron radii calculated from Eqs. (2b) and (30) for various glass compositions.

Composition mol % $\text{V}_2\text{O}_5$	$\epsilon_p^a$	$r_p$ (Å) from Eq. (2b)	$r_p$ (Å) from Eq. (30)
80.2	5.7	1.93	1.58
70.2	4.6	1.96	1.63
60.5	3.9	2.05	1.68

<sup>a</sup>From Cole-Cole plot of the complex dielectric constants.

Eq. (30) using average vanadium ion separation as an estimate for  $R$  are shown in Table III, which shows that the experimental and theoretical values of  $r_p$  are comparable.

The low-temperature dc conductivity data can be well fitted to Mott's variable-range-hopping conductivity [Eq. (3)]. A semilogarithmic plot of the dc conductivity,  $\sigma$ , versus  $T^{-1/4}$  is shown in Fig. 5 for the vanadium germanate glass in the low-temperature region. The solid lines in Fig. 5 are the best fits of Eq. (3) to the experimental data. In the fitting procedure,  $\alpha$  and  $N(E_F)$  are used as variable parameters. It is noted that the fits are reasonable below  $\sim 150 \text{ K}$ . The values of  $\alpha$  and  $N(E_F)$  obtained from the best fits are shown in Table IV. It should be noted that the values of  $\alpha$  are consistent with the previous estimate of  $\alpha$  from the high-temperature electrical data. The values of  $N(E_F)$  are also reasonable for localized states.<sup>15</sup>

However, the temperature dependence of the dc conductivity in the intermediate temperature range cannot be met in the Mott model. The temperature dependence of the dc conductivity, similar to the Mott model, is also predicted by the Holstein model [Eq. (5)] in the high-temperature region for the adiabatic hopping limit. An independent check of the nature of hopping is also provided by this model [Eq. (6)]. The limiting value of  $J$  estimated from the right-hand side of (6), using the value of  $\nu_0$  and  $W_H \simeq W$  from Table II, at 400 K is in the range 0.033–0.036 eV for all compositions. An unambiguous decision as to whether the polaron hopping is in the adiabatic or nonadiabatic regime requires an estimate of  $J$ .

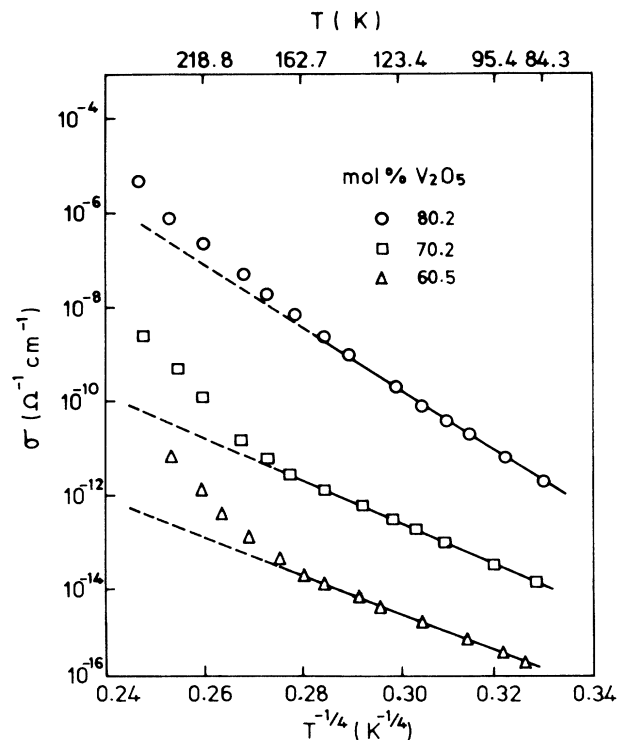


FIG. 5. The dc conductivity shown as a function of  $T^{-1/4}$  for three sample compositions (shown). The solid lines in the figure are fits to the variable-range-hopping model [Eq. (13)] for the values of the parameters shown in Table IV.

TABLE IV. Parameters obtained from the variable-range-hopping model at low temperatures for various sample compositions.

Sample composition mol % $V_2O_5$	$\alpha$ ( $\text{\AA}^{-1}$ )	$N(E_F)$ ( $\text{eV}^{-1} \text{cm}^{-3}$ )
80.2	1.14	$1.0 \times 10^{21}$
70.2	1.08	$2.5 \times 10^{21}$
60.5	1.03	$3.4 \times 10^{21}$

An upper limit can be deduced by assuming that the entire concentration dependence of the activation energy is due to the variation in  $J$ . For the present studies, this corresponds to a change in  $W$  from 0.32 to 0.44 eV (Table II), a possible variation in  $J$  being 0.12 eV. However, since  $W$  is likely to change with compositions, the true value is probably smaller than this. An independent estimate of  $J$  can also be made from the following expression:<sup>15</sup>

$$J \sim e^3 [N(E_F)/\epsilon_p^3]^{1/2}. \quad (31)$$

Using the previous estimate of  $N(E_F)$  (Table IV), Eq. (31) yields  $J \sim 0.1$  eV. Thus the adiabatic hopping theory may be the most appropriate to describe the polaronic conduction in the vanadium germanate glassy semiconductors.

The Schnakenberg model [Eq. (7)] predicts a temperature-dependent activation energy and Fig. 1 also shows temperature-dependent activation energy which decreases with decrease in temperature. Thus it appears that the Schnakenberg model might be appropriate for the vanadium germanate system. In Fig. 6,  $\log_{10}(\sigma T)$  is plotted as a function of reciprocal temperature. The theoretical curves given by Eq. (7) are also drawn in this figure, using  $\nu_0$ ,  $W_H$ , and  $W_D$  as variable parameters. The best fit to the experimental points, above the temperature of  $\sim 120$  K, has been observed for those values of the parameters shown in Table V. It may be noted that the value of  $\nu_0$  shows a little dispersion and is close to the value obtained from the infrared data.<sup>33</sup> As expected, the value of the hopping energy  $W_H$  is less than the high-temperature activation energy  $W$  (Table II). It should be noted that the values of  $W_D$  are close to the estimates of  $W_D$  from the Miller-Abrahams theory<sup>35</sup> for vanadate glasses. It might also be noted that the value of  $W_H + W_D/2$  is approximately equal to  $W$  in accordance with the prediction of the Mott model [Eq. (2a)]. However, the Schnakenberg model is not consistent with the dc conductivity data below 120 K.

Another model which accounts for the decrease of activation energy with decreasing temperature is due to Killias [Eqs. (8) and (9)]. In this model, the temperature-dependent activation energy [Eq. (9)] arises due to the dependence of the activation energy on the hopping distance.<sup>21</sup> Equation (9) predicted by this model indicates that the activation energy,  $W(T)$  is linearly dependent on the inverse temperature. However, the experimental activation energy estimated from Fig. 1 does not show in-

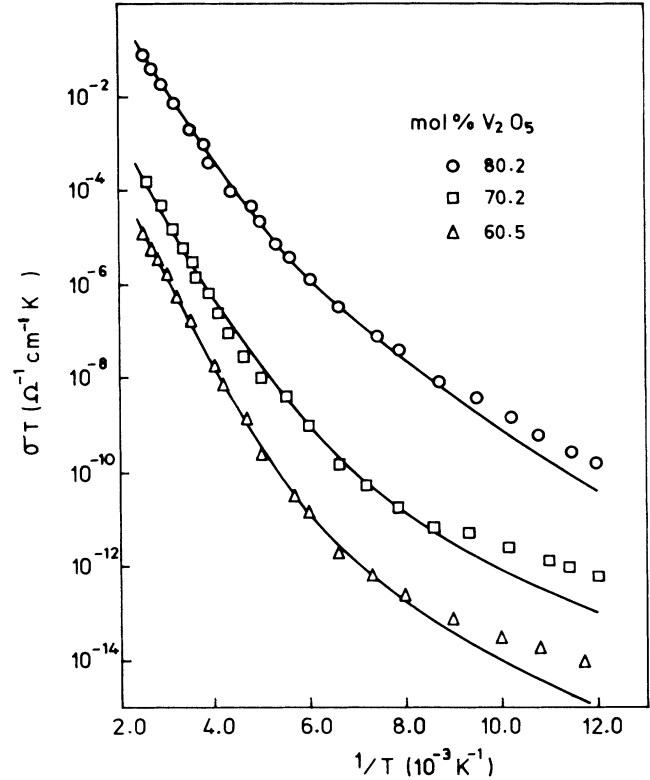


FIG. 6. Product of the dc conductivity and temperature ( $\sigma T$ ) shown as a function of reciprocal temperature. The solid curves are fits to Eq. (7) predicted by the Schnakenberg polaron model for the values of the parameters given in Table V.

verse temperature dependence, but rather follows Eq. (7) predicted by the Holstein model (Fig. 3).

## B. ac conductivity

### 1. Quantum-mechanical tunneling (QMT) model

The QMT model has been applied previously to the ac conductivity data for many amorphous semiconductors without much success, and it turns out the behavior of the vanadium germanate system reported here cannot be reconciled with this theory. The most obvious discrepancy between theory and experiment concerns the temperature dependence of the frequency exponent,  $s$  of the ac conductivity. From Eq. (15), the QMT model is seen, in its simplest form, to predict a value for  $s$  of  $\sim 0.81$  (for typical values of  $\omega$  and  $\nu_0$ ), which is temperature independent. However, it can be clearly seen from Fig. 4 that the

TABLE V. Parameters obtained by fitting the dc data to the Schnakenberg model for various sample compositions.

Glass composition mol % $V_2O_5$	$W_H$ (eV)	$W_D$ (eV)	$\nu_0$ ( $\text{s}^{-1}$ )
80.2	0.30	0.06	$9.6 \times 10^{12}$
70.2	0.34	0.08	$8.4 \times 10^{12}$
60.5	0.39	0.11	$7.2 \times 10^{12}$

frequency exponent  $s$  decreases with increasing temperature, thereby conflicting with the prediction of the simple QMT model. For the QMT model of nonoverlapping small polaron, i.e., for the NSPT model a temperature dependence of  $s$  is predicted, but it is of opposite sign [Eq. (16)]. The simple QMT model also predicts that  $s$  should decrease appreciably with increasing frequency.<sup>12</sup> No such variation is observed for the present glass system in the investigated frequency range ( $10^2$ – $10^5$  Hz) [Fig. 3(b)].

Nevertheless, the QMT model [Eq. (12)] suggests the temperature dependence of the ac conductivity in the form  $\sigma_1(\omega) \propto T^n$ , with  $n = 1$ . From the plot of  $\log_{10}\sigma_1(\omega)$  versus  $\log_{10}T$  (Fig. 7) for the germanate glass, it is observed that the ac conductivity increases linearly with temperature [i.e.,  $\sigma_1(\omega) \propto T^n$ , with  $n = 1$ ] over a considerable range of low temperature. However, at higher temperatures the ac conductivity starts to deviate from linearity, and the temperature at which deviation from linearity starts increases with increasing frequency. Fits to the experimental values of  $\sigma_1(\omega)$  made using Eq. (12) as a function of temperature are shown in Fig. 7 for lower temperatures. The values of the parameters obtained from the best fit are shown in Table VI. In the fitting procedure a fixed frequency ( $\omega = 10^4$  s<sup>-1</sup>) and a fixed value of the decay parameter ( $\alpha = 1.0$  Å<sup>-1</sup>) were assumed. It might be noted that the values of  $\tau_0$  obtained from the fitting procedure are approximately equal to the inverse phonon frequency  $\nu_0^{-1}$  estimated from the dc data (Table II). The values of  $N(E_F)$ , however, are lower by 1 order of magnitude than the estimates from the variable-hopping analysis (Table IV).

## 2. Overlapping-large-polaron tunneling (OLPT) model

The OLPT model predicts that  $\sigma_1(\omega)$  should have a negative temperature dependence of the frequency ex-

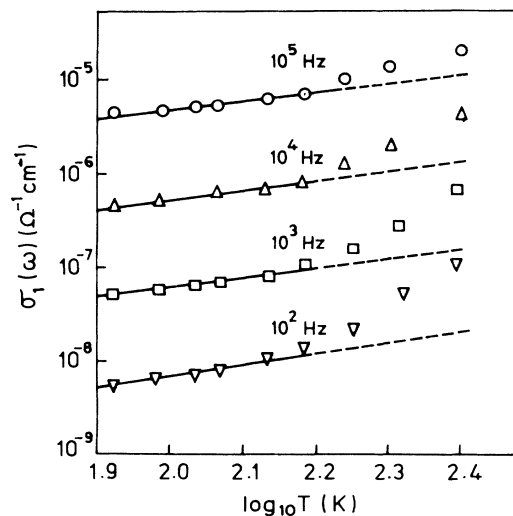


FIG. 7. Temperature dependence of the frequency-dependent conductivity (real part) obtained by the subtraction procedure as in Fig. 3(b) for the sample composition 80.2 mol %  $V_2O_5$ –19.8 mol %  $GeO_2$  plotted double logarithmically. The solid lines are the fits made using the QMT model [Eq. (12)].

TABLE VI. Parameters for various sample compositions, obtained by fitting low temperature ac data to the QMT model.

Sample composition mol % $V_2O_5$	$\tau_0$ (s)	$N(E_F)$ (eV <sup>-1</sup> cm <sup>-3</sup> )
80.2	$1.0 \times 10^{-13}$	$5.4 \times 10^{20}$
70.2	$1.7 \times 10^{-13}$	$2.3 \times 10^{20}$
65.5	$2.0 \times 10^{-13}$	$1.0 \times 10^{20}$

ponent  $s$ , at least at lower temperatures [Eq. (21)], and thus at first sight it appears that this model might be a possible contending theory to explain the data presented here. The theoretical curves for  $s$  predicted by the OLPT model [Eq. (21)] are drawn in Fig. 8 as a function of  $k_B T/W_{HO}$  for various values of the normalized polaron radius  $r'_0$ . These curves are universal in the sense that they are plotted versus reduced temperature,  $k_B T/W_{HO}$ , or put another way, changes in  $W_{HO}$  result in a rescaling of the temperature axis. The experimental data for  $s$  are fitted in Fig. 8, using  $W_{HO}$  as a variable parameter. The best fit to the experimental points is observed for the values of  $W_{HO}$  shown in Table VII. As is seen from Fig. 8, the experimental data for  $s$  lie between the theoretical curves for  $r'_0 = 1.0$  to 2.0 at low temperatures. However, at higher temperatures the experimental points neither reside between theoretical curves nor show minima as predicted by the OLPT model.<sup>13</sup>

Equation (18) can be used to estimate the large polaron radius  $r_0$  from the known values of the intersite separation  $R$  (Table I) and the previous estimate of the polaron hopping energy  $W_H$  (Table V). The estimated values of  $r_0$  (Table VII) are smaller than the average vanadium site separation and thus appear to be inconsistent with the basic premise of the overlapping large polarons.

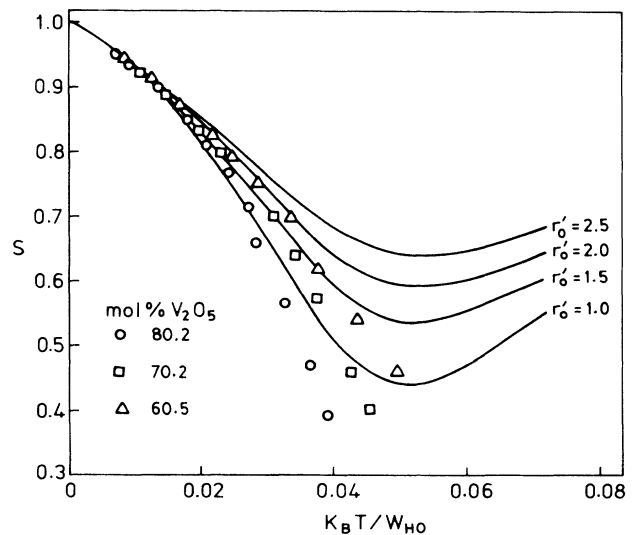


FIG. 8. The frequency exponent  $s$  for various sample compositions shown as a function of  $k_B T/W_{HO}$ . The solid curves are calculated from the OLPT model [Eq. (21)] for a fixed frequency  $\omega = 10^4$  s<sup>-1</sup> and relaxation time  $\tau_0 = 10^{-13}$  s and for various values of the normalized polaron radius  $r'_0$  (shown).

TABLE VII. Parameters obtained by fitting with the OLPT model at low temperatures for various sample compositions.

Sample composition mol % V <sub>2</sub> O <sub>5</sub>	$r'_0$	$W_{HO}$ (eV)	$r_0$ (Å)
80.2	1.0	1.02	2.70
70.2	1.5	1.17	2.87
60.5	2.0	1.31	2.92

The OLPT model [Eq. (21)] also predicts the frequency dependence of  $s$ . A detailed analysis shows that in the low-temperature region ( $k_B T/W_{HO} < 0.04-0.05$ ),  $s$  should increase with frequency. An opposite and more significant behavior should be observed in the high-temperature region ( $k_B T/W_{HO} > 0.05$ ). In the present work, the change in frequency did not exceed 3 orders of magnitude and the frequency dependence of  $s$  was not observed.

The OLPT model [Eq. (19)] predicts a considerably stronger temperature dependence of the ac conductivity in the temperature region where the frequency exponent  $s$  is a decreasing function of temperature. The functional form of the temperature dependence of  $\sigma_1(\omega)$  predicted by this model [Eq. (19)] is complicated and cannot be expressed simply as  $\sigma_1(\omega) \propto T^n$  with  $n$  constant over a considerable temperature range. Nevertheless, at low temperatures ( $k_B T/W_{HO} < 0.04-0.05$ ) the hopping length  $R_\omega$  has nearly constant temperature dependence,  $R_\omega \sim T^{1.25}$  (for  $r'_0 = 2.5$ ) and consequently  $\sigma_1(\omega) \propto T^6$  for the uncorrelated case, and also  $\sigma_1(\omega) \propto T^4$  for the correlated form of the OLPT model.<sup>13</sup> This is obviously at variance with the much weaker temperature dependence exhibited by the low-temperature data of the present work (Fig. 7).

### 3. Correlated barrier hopping (CBH) model

The CBH model [Eqs. (24) and (26)] predicts that  $\sigma_1(\omega)$  should behave, in some respects, in a similar manner to the OLPT model, namely it should have negative temperature dependence of the frequency exponent  $s$  and therefore it might be a possible candidate theory for the ac conduction in the present glass system.

A critical test for the CBH model comes from the temperature dependence of the ac conductivity and its frequency exponent  $s$ . Fits to the experimental values of  $s$  as a function of temperature made using Eq. (26) are shown in Fig. 4. The values of the parameters used in calculating the curves are those given in Table VIII. A fixed frequency ( $\omega = 10^4 \text{ s}^{-1}$ ) has been assumed in all cases. From Fig. 4, it is observed that the fit appears to be reasonable over the entire temperature range measured. In Fig. 3(a), the measured total conductivity  $\sigma_{tot}(\omega)$  is fitted to the measured values of the dc conductivity plus the ac conductivity calculated from Eq. (24) predicted by the CBH model, using  $W_M$  and  $\tau_0$  as variable parameters. The calculated curves are scaled so as to fit the value of  $\sigma_{tot}(\omega)$  at  $\omega = 10^5 \text{ s}^{-1}$  for the lowest temperature [i.e., thereby effectively fixing  $N$  (Table III)]. The values of  $W_M$  and  $\tau_0$

TABLE VIII. Parameters obtained by fitting with the CBH model for various sample compositions.

Sample composition mol % V <sub>2</sub> O <sub>5</sub>	$\tau_0$ (s)	$W_M$ (eV)	$N$ (cm <sup>-3</sup> )
80.2	$1.0 \times 10^{-12}$	0.95	$1.61 \times 10^{21}$
70.2	$3.1 \times 10^{-12}$	1.13	$1.87 \times 10^{21}$
60.5	$4.2 \times 10^{-12}$	1.29	$2.23 \times 10^{21}$

obtained by the fitting procedure for various sample compositions are collected in Table VIII. The values of  $W_M$  are, as expected, higher than the high-temperature activation energy for dc conduction. However, the values of the relaxation time  $\tau_0$  are higher than those that would be expected for typical inverse phonon frequency, although such a discrepancy is not unexpected when lattice relaxation effects are important.<sup>12</sup> It is also noted from Table VIII that the values of  $N$  obtained from this analysis are close to the concentrations of reduced vanadium ions estimated from ESR (Table I).

### C. Imaginary parts of the ac conductivity

The total measured capacitance  $C_{tot}(\omega)$ , like the conductance, can be decomposed into two components: a dispersive term  $C(\omega)$ , which arises due to loss mechanism, and a nondispersive term  $C_\infty$ , which is determined by the high-frequency atomic and dipolar vibrational transitions, viz.,

$$C_{tot}(\omega) = C(\omega) + C_\infty. \quad (32)$$

Several methods<sup>13</sup> for eliminating the nondispersive component exist, namely the numerical differentiation of the capacitance data, whereupon the constant term  $C_\infty$  drops out. Thus, if the dispersive part of the capacitance obeys the power law

$$C(\omega) \propto \omega^{s^1-1}, \quad (33)$$

(where  $s^1$  is different from  $s$ ) a plot of  $\log_{10}[-dC(\omega)/d \ln(\omega)]$  versus  $\log_{10}\omega$  should yield a straight line of slope  $s^1-1$ . This differentiation technique has been employed in the present work to determine  $C(\omega)$ . The ratio of the imaginary to the real part of the conductivity is then calculated from the relation

$$\sigma_2(\omega)/\sigma_1(\omega) = \omega C(\omega)/G(\omega), \quad (34)$$

where  $G(\omega)$  is the conductance at frequency  $\omega$ .

In Fig. 9, the experimental data for  $\sigma_2(\omega)/\sigma_1(\omega)$  [calculated from Eq. (34)] are plotted versus  $\log_{10}(\omega)$  for one glass composition at two temperatures. It is observed that  $\sigma_2(\omega)/\sigma_1(\omega)$  is temperature dependent. The QMT model [Eq. (27)] predicts a temperature-independent value for  $\sigma_2(\omega)/\sigma_1(\omega)$  and hence is not applicable to the data presented in Fig. 9. The temperature dependence of  $\sigma_2(\omega)/\sigma_1(\omega)$  predicted by the NSPT model [Eq. (28)] is also much weaker than the observed data shown (Fig. 9). On the other hand, the CBH model [Eq. (29)] predicts a stronger temperature dependence of  $\sigma_2(\omega)/\sigma_1(\omega)$ . In

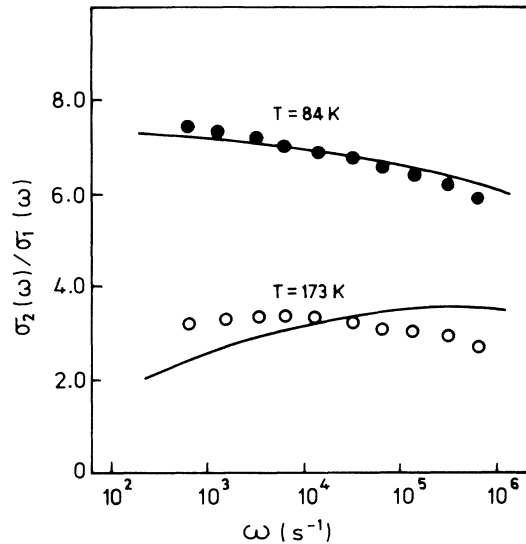


FIG. 9. Ratio of the imaginary to the real parts of the ac conductivity [ $\sigma_2(\omega)/\sigma_1(\omega)$ ] for the sample composition 80.2 mol %  $V_2O_5$ –19.8 mol %  $GeO_2$  at two temperatures shown as a function of frequency. The solid curves represents the behavior of the CBH model [Eq. (29)].

Fig. 9, the curves are shown corresponding to the predictions of the CBH model [Eq. (29)], using the same values of the parameters  $W_M$  and  $\tau_0$  (Table VIII) already deduced from the fitting of the real part of the conductivity to the CBH model [Eq. (24)]. The fit between theory and experiment may be regarded as good, bearing in mind that no extra parameters are used in the calculation of  $\sigma_2(\omega)/\sigma_1(\omega)$  from Eq. (29). The discrepancy is ascribed to the fact that Eq. (29) is only approximate; higher-order terms become important at high temperatures. It should be noted that the fits to  $\sigma_2(\omega)/\sigma_1(\omega)$  are very sensitive to the values of the parameters used (e.g.,  $W_M$  and  $\tau_0$ ) and

are more sensitive than the fits made to just the real part of the ac conductivity.

## VI. CONCLUSIONS

The dc conductivity as well as the real and imaginary parts of the ac conductivity for the vanadium germanate glassy semiconductors have been presented for the first time, in the temperature range 80–450 K and the frequency range  $10^2$ – $10^5$  Hz. Analysis of the observed dc data shows that at higher temperatures the dc conductivity is consistent with the predictions of the phonon-assisted hopping conduction model in the adiabatic approximation, while at low temperature the variable-range-hopping model is valid.

Of the various theoretical models for ac conduction in amorphous semiconductors (Sec. II), the CBH model is consistent with all aspects of the loss data, namely the temperature dependence of the ac conductivity and its frequency exponent. Fits using this model are in good agreement with the experimental data for all temperatures and frequencies measured. The other models, such as the QMT model, fail to predict the temperature dependence of the frequency exponent, although this model seems to be consistent with the low-temperature ac conductivity. The temperature dependence of the frequency exponent is in agreement with the predictions of the OLPT model in the low-temperature range, however, this model predicts a temperature dependence of the ac conductivity that is much stronger than the experimental data indicate.

Finally it should be remarked that fits to the ratio of the imaginary to the real parts of the conductivity are much more sensitive than fits to the real part of the conductivity alone.

## ACKNOWLEDGMENTS

The author is highly grateful to Professor D. Chakravorty, Indian Association for the Cultivation of Science, for helpful suggestions.

<sup>1</sup>N. F. Mott, *J. Non-Cryst. Solids* **1**, 1 (1968).

<sup>2</sup>I. G. Austin and N. F. Mott, *Adv. Phys.* **18**, 41 (1969).

<sup>3</sup>M. Sayer and A. Mansingh, *Phys. Rev. B* **6**, 4629 (1972).

<sup>4</sup>C. H. Chung and J. D. Mackenzie, *J. Non-Cryst. Solids* **42**, 151 (1980).

<sup>5</sup>A. E. Owen, *J. Non-Cryst. Solids* **25**, 370 (1977).

<sup>6</sup>A. Ghosh, *J. Phys. Condens. Matter* **1**, 7819 (1989), *Philos. Mag. B* **61**, 87 (1990).

<sup>7</sup>A. Ghosh and D. Chakravorty, *J. Phys. Condens. Matter* **2**, 931 (1990).

<sup>8</sup>A. Mansingh, R. P. Tandon, and J. K. Valid, *Phys. Rev. B* **21**, 4829 (1980).

<sup>9</sup>L. Murawski, *Philos. Mag. B* **50**, L69 (1984).

<sup>10</sup>A. Mansingh and V. K. Dhawan, *J. Phys. C* **16**, 1675 (1983).

<sup>11</sup>A. Ghosh, *Phys. Rev. B* **41**, 1479 (1990).

<sup>12</sup>S. R. Elliott, *Adv. Phys.* **36**, 135 (1987).

<sup>13</sup>A. R. Long, *Adv. Phys.* **31**, 553 (1982).

<sup>14</sup>N. F. Mott, *Philos. Mag.* **19**, 835 (1969).

<sup>15</sup>N. F. Mott and E. A. Davis, *Electronic Processes in Non-Crystalline Materials*, 2nd ed. (Clarendon, Oxford, 1979), p.

225.

<sup>16</sup>V. Ambegaokar, S. Cochran, and J. Kurkijarvi, *Phys. Rev. B* **8**, 3682 (1973).

<sup>17</sup>T. Holstein, *Ann. Phys. (N.Y.)* **8**, 343 (1959).

<sup>18</sup>D. Emin and T. Holstein, *Ann. Phys. (N.Y.)* **53**, 439 (1969).

<sup>19</sup>L. Friedman and T. Holstein, *Ann. Phys. (N.Y.)* **21**, 494 (1963).

<sup>20</sup>J. Schnakenberg, *Phys. Status Solidi* **28**, 623 (1968).

<sup>21</sup>H. R. Killias, *Phys. Lett.* **20**, 5 (1966).

<sup>22</sup>M. Pollak, *Philos. Mag.* **23**, 519 (1971).

<sup>23</sup>H. Bottger and V. V. Bryskin, *Phys. Status Solidi B* **78**, 415 (1976).

<sup>24</sup>P. N. Butcher and K. J. Hyden, in *Proceedings of the 7th International Conference on Amorphous and Liquid Semiconductors*, edited by W. E. Spear (Centre for Industrial Consultancy and Liaison, University of Edinburgh, 1977), p.234.

<sup>25</sup>A. L. Efros, *Philos. Mag. B* **43**, 829 (1981).

<sup>26</sup>M. Pollak, *Phys. Rev.* **138**, A1822 (1965).

<sup>27</sup>M. Pollak and G. E. Pike, *Phys. Rev. Lett.* **28**, 1449 (1972).

<sup>28</sup>G. Frössate, R. Maynard, R. Rummal, and D. Thoulouse, *J.*

- Phys. (Paris) Lett. **38**, L15 (1977).
- <sup>29</sup>G. E. Pike, Phys. Rev. B **6**, 1572 (1972).
- <sup>30</sup>S. R. Elliott, Philos. Mag. **36**, 1291 (1977).
- <sup>31</sup>S. R. Elliott, Philos. Mag. B **37**, 553 (1978).
- <sup>32</sup>S. R. Elliott, Philos. Mag. B **40**, 507 (1979); J. Non-Cryst. Solids **35-36**, 855 (1980).
- <sup>33</sup>Bh. V. Janakirama-Rao, J. Am. Ceram. Soc. **48**, 311 (1965).
- <sup>34</sup>V. N. Bogomolov, E. K. Kudinov, and Yu. A. Firsov, Fiz. Tverd. Tela (Leningrad) **9**, 3175 (1967) [Sov. Phys.—Solid State **9**, 2502 (1968)].
- <sup>35</sup>A. Miller and S. Abrahams, Phys. Rev. **120**, 745 (1960).